NQR, DSC, and X-Ray Structure Studies of Pyridinium Tetrabromozincate and Pyridinium Tetrabromocadmate $(C_5H_5NH)_2MBr_4 \cdot nH_2O$ (M = Zn and Cd; n = 0, 1); Phase Transitions and Weak Hydrogen Bond Interactions

Hideta Ishihara[a], Naoko Hatano[a], Keizo Horiuchi[b], Hiromitsu Terao[c], Ingrid Svoboda[d], and Hartmut Fuess[d]

[a] Faculty of Culture and Education, Saga University, Saga 840-8502, Japan
[b] Faculty of Science, University of the Ryukyus, 1 Senbaru, Okinawa 903-0213, Japan
[c] Faculty of Integrated Arts and Sciences, Tokushima University, Tokushima 770-8502, Japan
[d] Materials Science, University of Technology, Petersenstraße 23, 64287 Darmstadt, Germany

Reprint requests to Prof. H. Ishihara. E-mail: isiharah@cc.saga-u.ac.jp

Z. Naturforsch. **2011**, *66b,* 1261 – 1269; received September 6, 2011

Crystals of pyridinium tetrabromozincate and pyridinium tetrabromocadmate were obtained as monohydrates and anhydrous compounds. The crystal structure of metastable $(C_5H_5NH)_2CdBr_4 \cdot H_2O$ was determined at 300(2) K; triclinic space group $P\bar{1}$ with a = 7.875(2), b = 8.151(1), and c = 16.356(2) Å, α = 79.260(10), β = 86.030(10), and γ = 61.440(10)°, Z = 2. All compounds except for stable $(C_5H_5NH)_2CdBr_4 \cdot H_2O$ gave four ^{81}Br NQR lines at temperatures between 77 and around 325 K. The stable $(C_5H_5NH)_2CdBr_4 \cdot H_2O$ undergoes a first-order phase transition at T_c = 116 K. Four ^{81}Br NQR lines below T_c merged into two with equal intensities above T_c, indicating a 180° flip motion of water molecules in the r. t. phase. The ^{81}Br NQR lines of the two anhydrous compounds faded out around 325 K probably due to the reorientational motion of $ZnBr_4^{2-}$ or $CdBr_4^{2-}$ ions. The respective two ^{81}Br NQR lines of the hydrates exhibited anomalous positive temperature dependence. This is considered to be induced by a weakening in the interionic C-H···Br hydrogen bonds with increasing temperature. The DSC measurements of the anhydrous compounds have revealed phase transitions above r. t. The thermal behavior of $(C_5H_5NH)_2CdBr_4$ is complicated by the formation of metastable forms.

Key words: ^{81}Br NQR, DSC, Phase Transition, Pyridinium Tetrabromometalates, Crystal Structure, Weak Hydrogen Bonds

Introduction

The formation of a wide variety of complex compounds of $(AH)_2MBr_4$ (AH = substituted ammonium monocation; M = Zn, Cd) has been recorded. Although Zn and Cd belong to the group 12, there is a notable difference in their coordination behavior, *i. e.* the *harder* Lewis acid Zn^{2+} has a strong tendency to a tetrahedral coordination in $ZnBr_4^{2-}$, while the *softer* Lewis acid Cd^{2+} has a potential tendency to expand its coordination number from four to six so that an octahedral coordination in $CdBr_6^{2-}$ is often found in layers of $(CdBr_4^{2-})_\infty$. It seems interesting on the one hand to compare the crystal structures of the corresponding complex compounds of zinc and cadmium bromides with the same cations in order to understand the delicate building principle of the crystal structures depending on the combination of cations and anions. On the other hand, the importance of weak hydrogen bonds in the crystal structures has received much attention recently [1].

NQR (nuclear quadrupole resonance) spectroscopy is a powerful method to investigate the electronic distributions around relevant nuclei in crystalline solids and has been intensively used to study chemical bonding, crystal structures, and phase transitions *etc*. Hydrogen bonding interactions involving halogen atoms are known to become not infrequently detectable through the corresponding NQR frequencies and their temperature dependence. Thus, it may be worth while to elucidate the existence of weak hydrogen bonds such as C-H···Br in the present type of compounds

Table 1. ^{81}Br NQR frequencies at several temperatures.

Compounds	T (K)	— ν (MHz) —			
$(PyH)_2CdBr_4{\cdot}H_2O$ (**1s**)	77	70.20	68.69	57.77	55.64
(Stable form)	298	62.53	56.00	–	–
$(PyH)_2CdBr_4$ H_2O (**1m**)	77	66.33	62.34	61.53	61.13
(Metastable form)	281	64.03	57.52	61.79	61.67
$(PyH)_2CdBr_4$ (**2**)[a]	77	66.92	64.06	63.33	59.46
	269	64.62	61.60	61.84	58.83
$(PyH)_2ZnBr_4{\cdot}H_2O$ (**3**)	77	63.67	61.10	60.61	59.93
	280	61.87	60.38	60.37	58.00
$(PyH)_2ZnBr_4$ (**4**)[b–d]	77	64.73	61.99	61.33	58.05
	273	63.16	60.31	59.92	57.70

[a] The frequency values in ref. [15] are 66.867, 65.277, 64.778, and 64.102 MHz at 77 K, and 63.962, 63.097 and 61.675 MHz at r. t. (see text); [b] the frequency values in the Table are cited from ref. [12]; [c] the frequency values in ref. [15] are 64.829, 62.097, 61.390, and 58.016 MHz at liquid nitrogen temperature, and 62.750, 59.826, and 57.551 MHz at r. t. (see text); [d] the frequency values in ref. [16] are 61.182, 60.657, 59.801, and 57.944 MHz at 77 K, and 62.750, 59.826, and 57.559 MHz at 298 K (see text).

through NQR investigations. Weak interactions of this type may play an important role for the stabilization of crystal structures.

In the course of our studies on a series of complex compounds of cadmium and zinc bromides [2 – 14], we have measured the ^{81}Br NQR frequencies of pyridinium tetrabromocadmate(II) $(C_5H_5NH)_2CdBr_4$ and tetrabromozincate(II) $(C_5H_5NH)_2ZnBr_4$. Hiura [15] and Scaife [16] have already reported the ^{81}Br NQR frequencies of these compounds at both liquid nitrogen and r. t. Our frequency data have some discrepancies with theirs. In the process of trying to resolve the discrepancy, we have found the existence of hydrates of these compounds. In this paper we describe the temperature dependence of the ^{81}Br NQR frequencies of the title compounds. Further, thermal analyses and X-ray single-crystal diffraction were applied to elucidate the phase transitions and the bonding in the structures.

Results and Discussion

NQR frequencies and materials

The ^{81}Br NQR spectra have shown that monohydrates exist in addition to the anhydrous Zn and Cd compounds. Further, polymorphism was found in the case of the cadmium hydrate. The compounds investigated are abbreviated with the bold numbers in parentheses as follows: stable $(PyH)_2CdBr_4{\cdot}H_2O$ (**1s**), metastable $(PyH)_2CdBr_4{\cdot}H_2O$ (**1m**), $(PyH)_2CdBr_4$ (**2**), $(PyH)_2ZnBr_4{\cdot}H_2O$ (**3**), and $(PyH)_2ZnBr_4$ (**4**), where PyH stands for $C_5H_5NH^+$. The ^{81}Br NQR frequencies at representative temperatures are listed in Table 1. The frequencies for anhydrous $(PyH)_2ZnBr_4$ [15, 16] and $(PyH)_2CdBr_4$ [15] at liquid nitrogen and r. t. have already been reported. The values are given in the margin under Table 1. The frequency values of $(PyH)_2ZnBr_4$ in [15] are almost the same as the present results of **4**. The frequency values of the lower three of four lines for $(PyH)_2ZnBr_4$ at 77 K in [16] agree practically with those of the higher three of four lines for the hydrate **3**, but the remaining lines of both compounds contradict in frequencies. The frequencies of $(PyH)_2CdBr_4$ in [15] do not match with those of any Cd compounds of **1s** to **2**. The reason for these contradictory results is still unknown.

The temperature dependence of the ^{81}Br NQR frequencies (ν) is shown for **1s**, **1m** and **2** in Figs. 1, 2 and 3, respectively. That for **3** and **4** are shown together in Fig. 4. All the compounds except for **1s** gave four resonance lines throughout the measured temperature range. **1s** undergoes a phase transition at T_c = 116 K, and the low temperature phase (LTP) and the r. t. phase (RTP) are characterized by four and two resonance lines, respectively (Fig. 1). The ^{81}Br NQR signal intensities of **1s** in LTP were more than 5 times stronger than those in **1m**. The frequencies of the resonance lines of all compounds exist in the range of *ca.* 56 to 64 MHz at r. t. (Table 1). In our former studies on the crystal structures of a series of zinc and cadmium halide complexes [2 – 14], isolated tetrahedral anions were

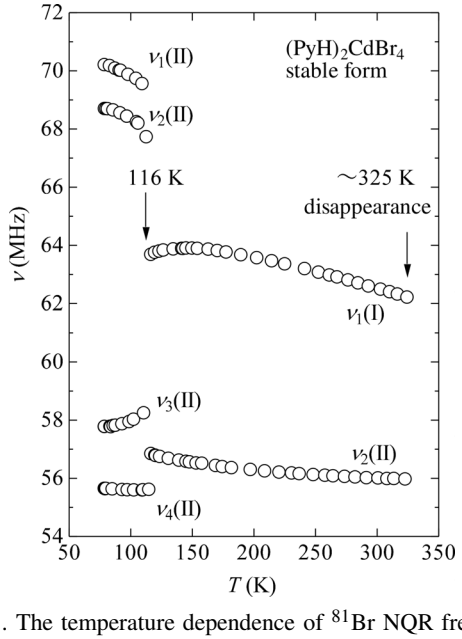

Fig. 1. The temperature dependence of ^{81}Br NQR frequencies of stable $(C_5H_5NH)_2CdBr_4{\cdot}H_2O$ (**1s**).

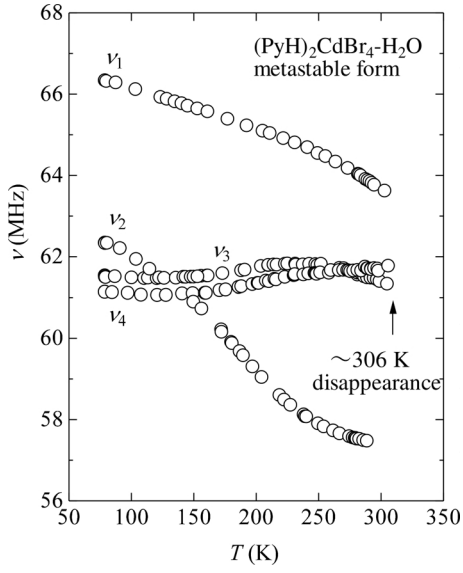

Fig. 2. The temperature dependence of ^{81}Br NQR frequencies of metastable $(C_5H_5NH)_2CdBr_4{\cdot}H_2O$ (**1m**).

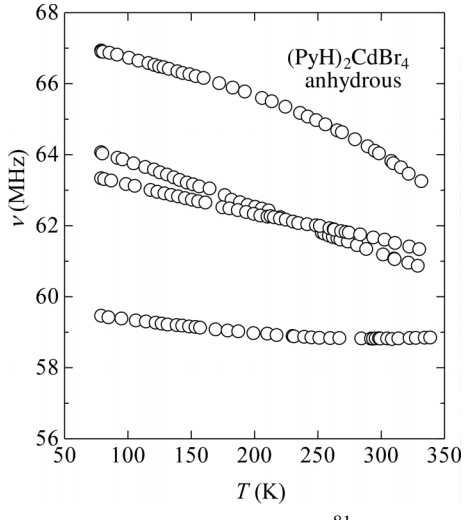

Fig. 3. The temperature dependence of ^{81}Br NQR frequencies of $(C_5H_5NH)_2CdBr_4$ (**2**).

solely found in the structures of the Zn compounds. By contrast, a variety of polymeric structures of anions have been found for the Cd compounds. Lower frequency lines are usually assigned to the Br atoms in M-Br-M bridges which are necessary in the formation of the polymeric structures. However, the ^{81}Br NQR frequencies of the present Cd compounds appear in a relatively narrow range with high frequencies being assignable to terminal Br atoms. Thus, isolated tetrahedral ions $ZnBr_4^{2-}$ or $CdBr_4^{2-}$ are expected to be

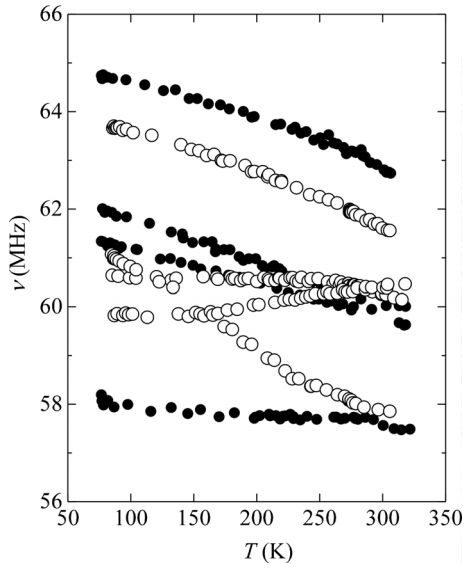

Fig. 4. The temperature dependence of ^{81}Br NQR frequencies of $(C_5H_5NH)_2ZnBr_4{\cdot}H_2O$ (**3**) (○) shown together with the published data of $(C_5H_5NH)_2ZnBr_4$ (**4**) (●) [12].

present in all crystals of these compounds. In accordance with this expectation, the X-ray structure investigation of **1m** has shown the existence of an isolated tetrahedral $CdBr_4^{2-}$ anion as described below.

X-Ray crystal structure study of a metastable form of $(PyH)_2CdBr_4{\cdot}H_2O$

The crystal structure has been determined for **1m**. The experimental conditions for the measurements and the crystal structure data are listed in Table 2 [17]. The unit cell is shown projected onto the *bc* plane in Fig. 5.

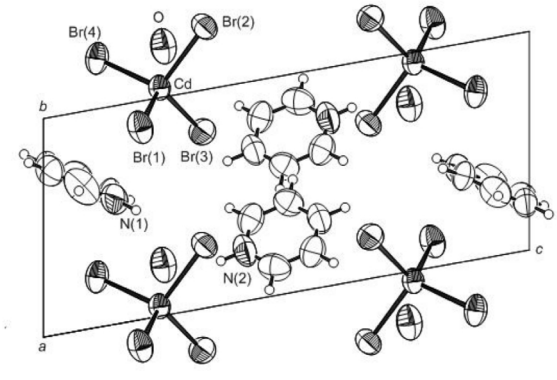

Fig. 5. The projection of the unit cell of metastable $(C_5H_5NH)_2CdBr_4{\cdot}H_2O$ (**1m**) along [100]. Displacement ellipsoids are drawn at the 50 % level, hydrogen atoms as spheres with arbitrary radii.

Table 2. Crystal structure data for metastable $(PyH)_2CdBr_4{\cdot}H_2O$ (**1m**).

Formula	$C_{10}H_{14}Br_4CdN_2O$
M_r	611.03
Crystal size, mm^3	$0.80 \times 0.35 \times 0.13$
Crystal system	triclinic
Space group	$P\bar{1}$
a, Å	7.875(2)
b, Å	8.151(1)
c, Å	16.356(2)
α, deg	79.26(1)
β, deg	86.03(1)
γ, deg	61.44(1)
V, $Å^3$	905.7(3)
Z	2
D_{calcd}, g cm^{-3}	2.23
$\mu(MoK_\alpha)$, cm^{-1}	100.2
$F(000)$, e	564
hkl range	$-11 \le h \le 3$, $-11 \le k \le 10$, $-22 \le l \le 22$
$((\sin\theta)/\lambda)_{max}$, $Å^{-1}$	0.7029
Refl. measured / unique / R_{int}	7377 / 5281 / 0.119
Refl. with $I \ge 2\sigma(I)$	2812
Param. refined	164
$R(F)$ / $wR(F^2)^{a,b}$ $[I \ge 2\sigma(I)]$	0.049 / 0.126
$R(F)$ / $wR(F^2)^{a,b}$ (all data)	0.119 / 0.155
GoF $(F^2)^c$	0.989
$\Delta\rho_{fin}$ (max / min), e $Å^{-3}$	1.03 / −1.12

[a] $R1 = \Sigma||F_o| - |F_c||/\Sigma|F_o|$; [b] $wR2 = [\Sigma w(F_o^2 - F_c^2)^2/\Sigma w(F_o^2)^2]^{1/2}$, $w = [\sigma^2(F_o^2) + (0.0844P)^2 + 0.3453P]^{-1}$, where $P = (\mathrm{Max}(F_o^2, 0) + 2F_c^2)/3$; [c] GoF $= [\Sigma w(F_o^2 - F_c^2)^2/(n_{obs} - n_{param})]^{1/2}$.

Table 3. Bond lengths and bond angles in metastable $(PyH)_2CdBr_4 \cdot H_2O$ (**1m**).

Bond	Distance (Å)	Connection	Angle (deg)
Cd-Br(1)	2.578(1)	Br(1)-Cd-Br(2)	107.49(4)
Cd-Br(2)	2.591(1)	Br(1)-Cd-Br(3)	111.25(4)
Cd-Br(3)	2.562(1)	Br(1)-Cd-Br(4)	112.28(3)
Cd-Br(4)	2.583(1)	Br(2)-Cd-Br(3)	106.73(3)
		Br(2)-Cd-Br(4)	107.50(3)
		Br(3)-Cd-Br(4)	111.27(4)

The asymmetric unit consists of two $C_5H_5NH^+$ ions, a $CdBr_4^{2-}$ ion and a water molecule. The bond lengths and angles in the cations are normal [17], and those in the anion are given in Table 3. The isolated $CdBr_4^{2-}$ ion is a slightly distorted tetrahedron with bond lengths from 2.56 to 2.59 Å and bond angles from 107 to 112°. The N-H···O and C-H···Br hydrogen bonds are listed in Table 4. The O-H···Br hydrogen bonds are also included in Table 4, even though they are a little longer than the sum of the van der Waals radii within 0.1 Å. The O-H···Br(4) hydrogen bond may be stronger than the O-H···Br(1) one by judging from the O···Br distances. The water oxygen

Table 4. Hydrogen bonds and short contacts in metastable $(PyH)_2CdBr_4 \cdot H_2O$ (**1m**).

D-H···A	d(D-H) (Å)	d(H···A) (Å)	D(D···A) (Å)	∠D-H···A (deg)
N(1)-H(N1)···O	0.86	2.34	3.088(13)	146
N(2)-H(N2)···O	0.86	2.03	2.808(9)	150
O-H···Br(1)	–	–	3.429(8)	–
O-H···Br(4)	–	–	3.343(8)	–
C(1)-H(C1)···Br(2)	0.93	2.88	3.642(10)	141
C(10)-H(C10)···Br(3)	0.93	2.90	3.671(10)	141

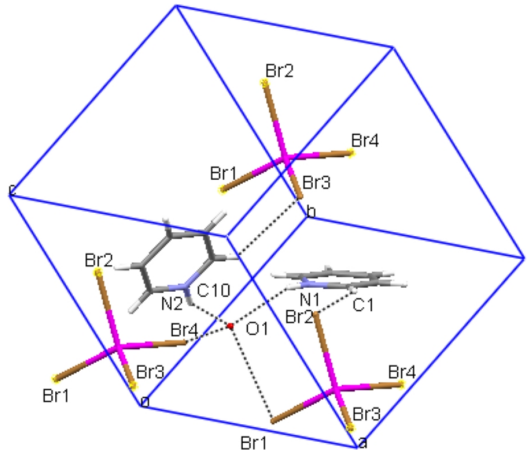

Fig. 6 (color online). The tetrahedral coordination of the oxygen atom of a water molecule in the crystal structure of metastable $(C_5H_5NH)_2CdBr_4{\cdot}H_2O$ (**1m**). The oxygen atom of the water molecule is surrounded by two nonequivalent cations and two equivalent anions. The dotted lines show the hydrogen bonding interactions. See Table 4 for numbers pertinent to hydrogen bonds and short contacts.

atom is surrounded tetrahedrally by two cations and two anions through N-H···O and O-H···Br hydrogen bonds, respectively, as shown in Fig. 6. On the other hand, the cation and the anion are connected to each other through C-H···Br(2) and C-H···Br(3) hydrogen bonds with almost similar strength according to their hydrogen bond lengths.

Anomalous temperature dependence of ^{81}Br NQR frequencies and hydrogen bond interactions

The appearances of the ν *vs.* T curves of the anhydrous compounds **2** and **4** resemble each other (Figs. 3 and 4). The two resonance lines with middle frequencies are situated in proximity, and the other two lines are situated above and below with roughly the same frequency separations. The resemblance between the ν *vs.* T curves of the hydrates **1m** and **3** is also quite noticeable (Figs. 2 and 4). The highest frequency lines

show normal negative temperature dependence, but the temperature behavior of the remaining three lines is unusual. These resemblances between the ν *vs.* T curves suggest that the pairs of the anhydrous and hydrated compounds are isomorphous.

The Bayer theory [18] predicts that NQR frequencies decrease monotonously owing to the increased librational motions with increasing temperature. However, the NQR frequencies of atoms with intermolecular bonds often show anomalous positive or only very slight temperature dependence. This reason is usually ascribed to a change in their intermolecular bonds caused by the increasing molecular motions with temperature. Another effect of intermolecular bonds generally observed is a lowering in the frequencies, which is due to the decrease of unbalanced p electron numbers of the relevant atom compared to a state free from intermolecular bonding.

As described above, the Br(2) and Br(3) atoms of **1m** participate in weak C-H···Br hydrogen bonds with the cations (Fig. 6). Further, the Br(1) and Br(4) atoms may participate in weak O-H···Br hydrogen bonds with water. Therefore, the anomalous temperature dependence of the ^{81}Br NQR frequencies observed for **1m** should be related to Br atoms participating in hydrogen bonds. On the other hand, the water molecule also participates in hydrogen bonds O-H···N with the cations. The consideration of the situation leads to the following assignments. First, the similarity in strength between the C-H···Br(2) and C-H···Br(3) hydrogen bonds indicates that ν_3 and ν_4 are assignable to Br(2) and Br(3) or *vice versa*. Thus, the slight and buoyant temperature dependence of ν_3 and ν_4 is explained as a result of weakening C-H···Br(2) and C-H···Br(3) hydrogen bonds caused by the increased motion of the cations with increasing temperature. The motions of the cations must be correlated with those of water molecules attached through the O-H···N hydrogen bonds. Second, by considering that the O-H···Br(4) hydrogen bond is stronger than the O-H···Br(1) hydrogen bond, the lowest frequency line at r. t., ν_2, may be assigned to Br(4). Thus, while the O-H···N hydrogen bonds are weakened as described above, the O-H···Br(4) hydrogen bonds may be strengthened conversely with the increasing motions of the water molecules. Lastly, the highest frequency line, ν_1, may be assigned to Br(1). It is supposed that the O-H···Br(1) hydrogen bonds are quite weak throughout the measured temperature range.

In an extension of the above assignments, the two proximate ^{81}Br NQR lines at middle frequencies in **2** are also assigned to Br atoms engaged in C-H···Br hydrogen bonds because of the similar ^{81}Br NQR frequencies for **1m** and **2** at r. t. In this case, the normal temperature dependence of these lines is explainable by lack of a weakening of the C-H···Br hydrogen bonds. On the other hand, the Br atoms assigned to the remaining two lines may be engaged in N-H···Br hydrogen bonds with cations instead of O-H···Br bonds with water. The similarities in the ν *vs.* T curves between the respective pairs of the hydrates **1m** and **3** and the anhydrous compounds **2** and **4** suggest that weak hydrogen bonds such as C-H···Br, N-H···Br, O-H···Br, and O-H···N exist also in the Zn compounds.

The NQR signals of all compounds showed the fade-out slightly above r. t., *viz.* around 324, 306, 340, 318, and 324 K for **1s**, **1m**, **2**, **3**, and **4**, respectively, far below the melting points. The fade-outs in the hydrates may be due to dehydration as stated below. However, the fade-outs in the anhydrous compounds may be ascribed to the activation of reorientational motions of the anions $M\mathrm{Br_4}^{2-}$ as stated below.

Low-temperature phase transition in the stable form of $(PyH)_2CdBr_4{\cdot}H_2O$

The temperature dependence of the ^{81}Br NQR frequencies shows that the symmetry of **1s** is lowered during the phase transition from RTP to LTP at T_c = 116 K (Fig. 1). The RTP structure is characterized by two ^{81}Br NQR lines with the same intensity, implying that the $\mathrm{CdBr_4}^{2-}$ ion has a symmetry plane or a 2-fold axis. On the other hand, LTP is characterized by four ^{81}Br NQR lines with the same intensity, showing an asymmetry of the $\mathrm{CdBr_4}^{2-}$ ion. A wider frequency range of the resonance lines in LTP than in RTP indicates an increased distortion of the $\mathrm{CdBr_4}^{2-}$ tetrahedron. Each resonance line in RTP splits discontinuously into two lines in LTP, indicating that the transition is a first-order type. Moreover, the DTA curves of **1s** show representative exothermic and endothermic anomalies in the cooling and heating runs, respectively (Fig. 7). However, the phase transition temperature at 109 K (on heating) observed by DTA is significantly lower than at T_c = 116 K observed by NQR. This fact may show that the phase transition temperature is quite dependent on the measuring processes with supercooling.

Though the crystal structure of **1s** has not yet been clarified, the easiness of the transformations from **1m**

Compounds	Transitions	T_c (K)	ΔH (kJ mol^{-1})	ΔS (J K^{-1} mol^{-1})	ΔT_c (K)
$(PyH)_2CdBr_4{\cdot}H_2O$(**1m**)	III → II[a]	331	16.6	50.2	–
	II → I[a]	358	2	6	–
	I → liquid[a]	436	19.9	45.6	–
	III′ → II′[b]	356	4.5	13	73
	II′ → I′[b]	429	–	–	52
	I′ → liquid[b]	436	28.4[f]	65[f]	35
$(PyH)_2CdBr_4$ (**2**)	III → II[c]	356	4.8	13	–
	II → I[c]	424	0.1	0.2	–
	I → liquid[c]	435	25.4	58.4	27
	III′ → I[d]	341	4.4	13	28
	III″ → II[e]	337	5.1	15	34
$(PyH)_2ZnBr_4{\cdot}H_2O$ (**3**)[g]	II → I[h]	340	15	44	8
$(PyH)_2ZnBr_4$ (**4**)[i]	II → I	342	6.3	18	43
	I → liquid	448	28	62	25

Table 5. Transition points T_c, transition enthalpies ΔH, and transition entropies ΔS, the temperature differences ΔT_c in between heating and cooling runs.

[a,b,c,d,e] The suffixes represent the heating runs affixed with the corresponding letters in the schematic DSC curves shown in Fig. 5; [f] the sums correspond to II′ → I′ and I′ → liquid; [g] with sealed pan; [h] ref. [13]; [i] this thermal anomaly was accompanied by another lengthy one (see text).

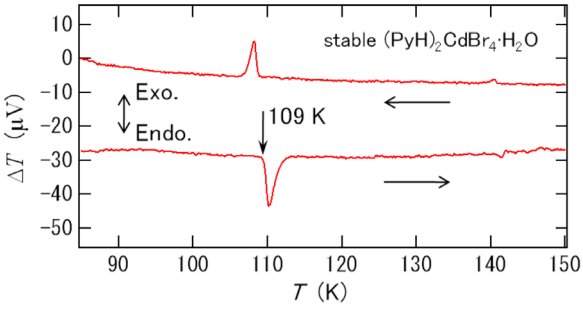

Fig. 7 (color online). DTA curves for stable $(C_5H_5NH)_2CdBr_4{\cdot}H_2O$ (**1s**).

to **1s** and *vice versa*, in addition to the closeness of their ^{81}Br NQR frequencies, indicates that their crystal structures are closely related. The high-frequency line ν_1(I) in RTP of **1s** is near 62 MHz which is almost equal to the two middle-frequency lines ν_3 and ν_4 of **1m** at r. t. This suggests that ν_1(I) may be assigned to two equivalent Br atoms which take part in two *symmetric* C-H···Br bonds in the crystal of **1s**. On the other hand, the low-frequency line ν_2(I) of RTP is lower by about 1 MHz than the lowest line ν_2 of **1m** at r. t. The slight temperature dependence of ν_2(I) is in contrast to the strong dependence of ν_2. This fact may be understandable by postulating that the two equivalent Br atoms of ν_2(I) are involved in two *symmetric* O-H···Br bonds with water, the strength of which is greater than that of the corresponding *asymmetric* O-H···Br(4) and O-H···Br(1) bonds in **1m**. The stronger hydrogen bonds in **1s** are reflected by the disappearance temperature of the NQR lines *ca.* 20 K higher compared to **1m** as described above.

Four ^{81}Br NQR lines in LTP of **1s** show that both O-H···Br and C-H···Br hydrogen bonds become asymmetrical in this phase. It is characteristic that the averaged frequency of ν_3(II) and ν_4(II) is preserved to be almost equal to the frequency of ν_2(I) at T_c, showing that the average strength of O-H···Br hydrogen bonds is almost same in both phases at this temperature. This is indicative of a 180° flip motion of water molecules leading to virtually symmetric O-H···Br contacts in RTP; the restriction of this motion in LTP results in the formation of stronger and weaker O-H···Br hydrogen bonds. On the other hand, both ν_1(II) and ν_2(II) in LTP split to the high frequency side in the extension of the ν_1(I) *vs.* T curve in RTP. This fact may reflect the rearrangement of the cations from the configuration with two different, quite weak C-H···Br hydrogen bond in LTP to that with two equivalent stronger ones under the 180° flip motion of the water molecules in RTP.

DSC study and phase transitions at higher temperatures

We have already reported the results of DSC measurements for **4** [13], which showed a phase transition at 342 K. The results of new DSC measurements are listed in Table 5 together with those for **4**. None of the compounds in the Table did exhibit any heat anomalies between 130 K and r. t. An anomaly for **2** corresponding to that of **4** was found at 356 K showing the occurrence of phase transitions related to the reorientational motions of MBr_4^{2-} as observed in the series of compounds $[N(CH_3)_4]_2MX_4$ (M = Zn, Cd, Hg; X = Cl, Br, I) [8, 19].

A schematic drawing of the DSC curve of **2** is shown in Fig. 8a. An endothermic heat anomaly was observed at $T_{III\rightarrow II}$ = 356 K in the first heating run up to 413 K. In the second heating run made immediately after the cooling run (see run e in Fig. 8a), the starting temper-

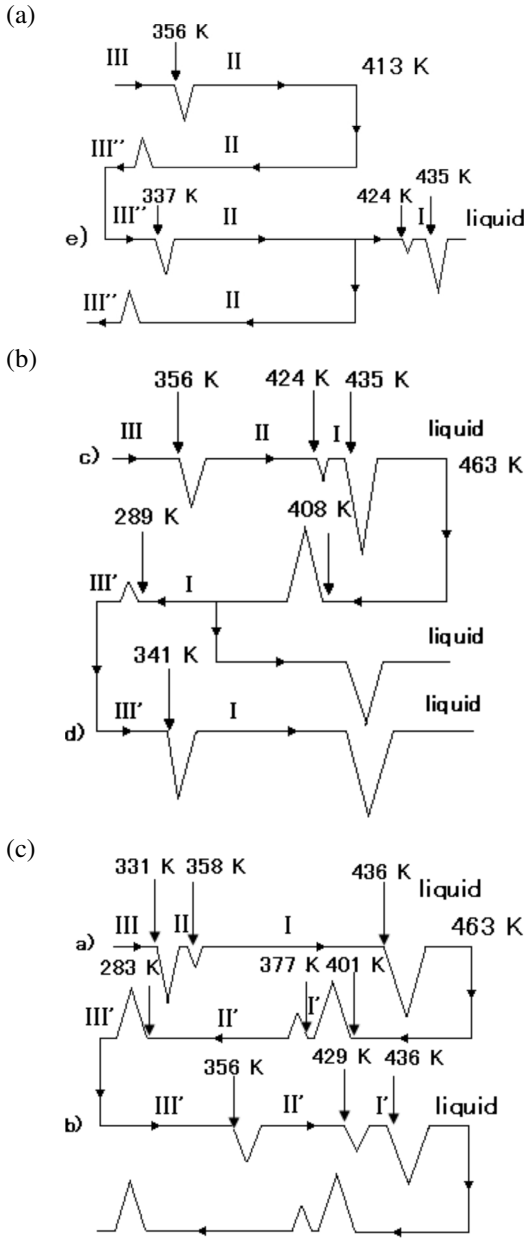

Fig. 8. Schematic DSC curves of the Cd compounds: (a) for $(PyH)_2CdBr_4$ (**3**) heating up to 413 K (below T_{II-I}) in the first heating run, (b) for $(PyH)_2CdBr_4$ (**3**) heating up to the melting point in the first heating run, and (c) for metastable $(PyH)_2CdBr_4{\cdot}H_2O$ (**1m**).

ature of the anomaly was lowered to $T_{III''\rightarrow II}$ = 337 K. However, the measurements done for an aged sample, kept at r. t. for several days after the $T_{III''\rightarrow II}$ transition, restored exactly the same results with 356 and 337 K for $T_{III\rightarrow II}$ and $T_{III''\rightarrow II}$, respectively, as for the virgin sample. Further, when the first heating run was extended to 463 K, an additional small heat anomaly appeared at $T_{II\rightarrow I}$ = 424 K just below the melting point T_m = 435 K (see run c in Fig 8b). In the successive cooling run to r. t., not two but a single exothermic peak anomaly emerged at 289 K. As shown in run d in Fig. 8b, the reheating run to a temperature above T_m executed immediately after cooling did not produce the above small heat anomaly peak of $T_{II\rightarrow I}$ but a single heat anomaly at $T_{III'\rightarrow I}$ = 341 K. The aged sample, kept for several days at r. t. after melting, recovered the same peak anomaly with $T_{III\rightarrow II}$ = 356 K and $T_{II\rightarrow I}$ = 424 K as for the virgin sample. The above observations show that **2** can exist in at least two r. t. metastable phases, III′ and III″, in addition to the stable phase III.

The DSC curves of **1m** obtained from an open pan are shown in Fig. 8c. The first heating run to above T_m showed a two-step dehydration at 331 and 358 K. The remeasurement results for this sample cooled to room temperature were similar to those in Fig. 8b for **2**, with a small difference in the temperature of the anomaly: $T_{III'\rightarrow II'}$ = 356 K and $T_{II'\rightarrow I'}$ = 429 K in **1m** correspond to $T_{III\rightarrow II}$ = 356 K and $T_{II\rightarrow I}$ = 424 K in **2** indicating the formation of the anhydrous form **1m** without decomposition. However, there were some differences between the original **2** and the dehydrated sample of **1m** in the second heating runs. In the case of the original **2** the lowest endothermic peak anomaly appeared at $T_{III\rightarrow II}$ = 356 K in the first run, but it appeared at $T_{III'\rightarrow I}$ = 341 K in the repeated run owing to the appearance of a metastable state III′ (Fig. 8b). In the case of the dehydrated sample of **1m** the lowest peak was always $T_{III'\rightarrow II'}$ = 356 K, even in the repeated measurements (Fig. 8c). In addition, the small anomaly at $T_{II'\rightarrow I'}$ and the corresponding exothermal anomaly at $T_{I'\rightarrow II'}$ appeared inevitably in each run for the dehydrated sample of **1m** (Fig. 8c). On the contrary, the corresponding anomaly at $T_{II\rightarrow I}$ for the original **2** was found only in the first run and the exothermal counterpart was not found in the successive cooling run (Fig. 8b). These observations suggest that the metastable states do not appear for the dehydrated sample of **1m** probably owing to the existence of a small amount of water remaining in the sample even after dehydration and successive melting.

4 showed a heat anomaly at 342 K before melting at 448 K in the heating run [13]. The present DSC measurements of **3** in sealed pans again showed a heat anomaly around 340 K, but accompanied with a lengthy sluggish anomaly between 410 and 420 K in

a heating run. A similar DSC curve was also observed for **1m** in the measurement with a sealed pan. In this case a heat anomaly at 332 K was followed by a broad anomaly skirted up to *ca.* 390 K. These observations indicate a time-consuming dehydration of the samples.

Conclusion

The crystal structure of the metastable form **1m** has been determined by single-crystal X-ray diffraction. The water molecules connect the cations and anions through N-H···O and O-H···Br hydrogen bonds, respectively, while the cations and anions are directly connected through C-H···Br hydrogen bonds. The ^{81}Br NQR frequencies of the respective two middle-frequency lines of both **1m** and **3** exhibit an anomalously small and partly positive temperature dependence, which may be explained by the weakening of the C-H···Br hydrogen bonds associated with the increased motions of the water molecules with increasing temperature. The lowest-frequency ^{81}Br NQR lines of the above two compounds at r. t. exhibit anomalously large negative temperature dependence, suggesting that a strengthening in one of two O-H···Br hydrogen bonds of the water molecule occurs with increasing temperature. The stable form **1s** undergoes a first-order phase transition between the LTP and RTP structures at 116 K; a 180° flip-flop motion of water molecules appears to be allowed in RTP, which is restricted in LTP. Both **2** and **4** undergo phase transitions near r. t., which may be related to reorientational motions of the anions $M\mathrm{Br_4}^{2-}$. **2** undergoes another phase transition below the melting point, which is absent in successive runs owing to the appearance of metastable states at r. t. The present results demonstrate that the temperature dependence of ^{81}Br NQR frequencies is sensitive to the dynamical changes in the weak hydrogen bonds such as C-H···Br which complement the stronger N-H···Br and O-H···Br interactions.

Experimental Section

Materials

The hydrous compounds of **1m** and **3** were obtained by concentrating hydrobromic acid solutions containing a 2 : 1 molar ratio of pyridine and $ZnBr_2$ or $CdCO_3$ over NaOH in a desiccator. The anhydrous compounds **2** and **4** were obtained by drying the hydrous ones over P_2O_5 in a desiccator. It was observed by ^{81}Br NQR spectroscopy that **1m** transformed to **1s** within several months at r. t. The transformation was accelerated by cooling to *ca.* 190 K. The transformation of **1s** to **1m** was achieved by heating to *ca.* 350 K and subsequent cooling to r. t. – Elemental analyses: For **1m**: calcd. C 19.68, H 2.31, N 4.59; found C 19.99, H 2.07, N 4.66; for **2**: calcd. C 20.28, H 2.04, N 4.73; found C 20.22, H 2.06, N 4.73; for **3**: calcd. C 21.32, H 2.51, N 4.97; found C 21.72, H 2.32, N 5.07; for **4**: calcd. C 22.02, H 2.21, N 5.13; found C 21.98, H 2.24, N 5.16. The analysis result for **3** seems to fit to the hemihydrate $(PyH)_2ZnBr_4 \cdot 1/2H_2O$ with smaller errors. However, the TG measurement of **3** showed the weight loss from around 340 K to near the melting point to be 3.2 %, which is consistent with the value of 3.2 % from the chemical formula. Further, we measured directly the weight gain for the anhydrous to form the hydrate and *vice versa* using a conventional analytical balance: The anhydrous form was obtained by drying wet crystals of hydrates for a long time to a constant weight at 353 K in an electric oven. The anhydrous one was then kept with water in a desiccator until a constant weight was reached. The weight increase corresponded to the monohydrate. It was noticed that the volume of the crystals expanded considerably during hydration. The crystals gave the ^{81}Br NQR signals of **1m**. Crystals of the hydrate were dehydrated again to a constant weight at 353 K in an electric oven, the results being consistent with the dehydration of a monohydrate.

Measurements

The structure of **1m** was determined using a four-circle X-ray diffractometer Nonius CAD4 (MoK_α radiation, λ = 0.7109 Å, graphite monochromator) [17]. All calculations were performed using the SHELX-97 program package [20].

The ^{81}Br NQR spectra were observed by using a home-made super-regenerative type oscillator. The resonance frequencies were determined by a counting method. The accuracy of the frequency measurements is estimated to be within $\pm$0.05 MHz. The DSC measurements were performed above 130 K with a differential scanning calorimeter DSC220 from Seiko Instruments Inc. under the following conditions: sample weights *ca.* 10 mg, heating or cooling rates 2 – 10 K min^{-1} under flowing dry N_2 gas at 40 mL min^{-1}. TG measurements were carried out by using a Rigaku Instrument TAS100 (TG-DTA/S); sample weights *ca.* 10 mg, heating rates 10 K min^{-1} under flowing dry N_2 gas at 10 mL min^{-1}. Low-temperature DTA measurements were performed by using a home-made apparatus.

[1] G. R. Desiraju, T. Steiner, *The Weak Hydrogen Bond in Structural Chemistry and Biology*, Oxford University Press, New York, **1999**.
[2] H. Ishihara, V. G. Krishnan, S. Dou, A. Weiss, *Z. Naturforsch.* **1994**, *49a*, 213 – 222.
[3] H. Ishihara, S. Dou, K. Horiuchi, V. G. Krishnan, H. Paulus, H. Fuess, A. Weiss, *Z. Naturforsch.* **1996**, *51a*, 1027 – 1036.
[4] H. Ishihara, S. Dou, K. Horiuchi, V. G. Krishnan, H. Paulus, H. Fuess, A. Weiss, *Z. Naturforsch.* **1996**, *51a*, 1216 – 1228.
[5] H. Ishihara, S. Dou, K. Horiuchi, H. Paulus, H. Fuess, A. Weiss, *Z. Naturforsch.* **1997**, *52a*, 550 – 560.
[6] H. Ishihara, K. Horiuchi, T. M. Gesing, S. Dou, J. C. Buhl, H. Paulus, H. Fuess, *Z. Naturforsch.* **1998**, *53a*, 717 – 724.
[7] H. Ishihara, K. Horiuchi, S. Dou, T. M. Gesing, J. C. Buhl, H. Paulus, I. Svoboda, H. Fuess, *Z. Naturforsch.* **1999**, *54a*, 628 – 636.
[8] H. Ishihara, K. Horiuchi, T. M. Gesing, S. Dou, J. C. Buhl, H. Terao, *Z. Naturforsch*. **2000**, *55a*, 225 – 229.
[9] H. Ishihara, K. Horiuchi, V. G. Krishnan, I. Svoboda, H. Fuess, *Z. Naturforsch*. **2000**, *55a*, 390 – 396.
[10] K. Horiuchi, H. Ishihara, H. Terao, *J. Phys. Condens. Matter.* **2000**, *12*, 4799 – 4806.
[11] H. Ishihara, T. Okajima, K. Horiuchi, I. Svoboda, H. Fuess, *Z. Naturforsch*. **2000**, *56a*, 641 – 646.
[12] H. Ishihara, N. Hatano, K. Horiuchi, H. Terao, *Z. Naturforsch.* **2002**, *57a*, 343 – 347.
[13] K. Horiuchi, H. Ishihara, N. Hatano, S. Okamoto, T. Gushiken, *Z. Naturforsch*. **2001**, *57a*, 425 – 430.
[14] H. Ishihara, K. Horiuch, T. M. Gesing, J. C. Buhl, P. Erk, *Z. Naturforsch*. **2002**, *57b* 503 – 508.
[15] M. Hiura, *J. Sci. Hiroshima Univ.* **1982**, *A45*, 383 – 405.
[16] D. E. Scaife, *Aust. J. Chem.* **1971**, *24*, 1315 – 1323.
[17] CCDC 697091 contains the supplementary crystallographic data for this paper. These data can be obtained free of charge from The Cambridge Crystallographic Data Centre *via* www.ccdc.cam.ac.uk/data_request/cif.
[18] H. Bayer, *Z. Physik* **1951**, *130*, 227 – 238; D. Nakamura, T. Ikeda, M. Kubo, *Coord. Chem. Rev.* **1975**, *17*, 281 – 316.
[19] H. Terao, T. Okuda, K. Yamada, H. Ishihara, A. Weiss, *Z. Naturforsch.* **1996**, *51a*, 755 – 760.
[20] G. M. Sheldrick, SHELXS/L-97, Programs for Crystal Structure Determination, University of Göttingen, Göttingen (Germany) **1997**. See also: G. M. Sheldrick, *Acta Crysrallogr*. **1990**, *A46*, 467 – 470; *ibid*, **2008**, *A64*, 112 – 122.